Published in final edited form as:
Cancer Res. 2010 December 1; 70(23): 9886–9894. doi:10.1158/0008-5472.CAN-10-1419.

Increase of plasma VEGF after intravenous administration of bevacizumab is predicted by a pharmacokinetic model

Marianne O. Stefanini[1], **Florence T.H. Wu**[1], **Feilim Mac Gabhann**[2], and **Aleksander S. Popel**[1]

[1] Department of Biomedical Engineering, Johns Hopkins University School of Medicine, Baltimore, MD

[2] Institute for Computational Medicine and Department of Biomedical Engineering, Johns Hopkins University, Baltimore, MD

Abstract

Vascular endothelial growth factor (VEGF) is one of the most potent cytokines targeted in anti-angiogenic therapies. Bevacizumab, a recombinant humanized monoclonal antibody to VEGF, is being used clinically in combination with chemotherapy for colorectal, non-small cell lung and breast cancers, and as a single agent for glioblastoma, and is being tested for other types of cancer in numerous clinical trials. It has been reported that the intravenous injection of bevacizumab leads to an increase of plasma VEGF concentration in cancer patients. The mechanism responsible for this counterintuitive increase has not been elucidated, although several hypotheses have been proposed. We use a multiscale systems biology approach to address this problem. We have constructed a whole-body pharmacokinetic model comprising three compartments: blood, normal tissue and tumor tissue. Molecular interactions between VEGF-A family members, their major receptors, the extracellular matrix, and an anti-VEGF ligand are considered for each compartment. Diffusible molecules extravasate, intravasate, are removed from the healthy tissue through the lymphatics, and are cleared from the blood. Our model reproduces the experimentally-observed increase of plasma VEGF following intravenous administration of bevacizumab, and predicts this increase to be a consequence of inter-compartmental exchange of VEGF, the anti-VEGF agent and the VEGF/anti-VEGF complex. Our results suggest that a fraction of the anti-VEGF drug extravasates, allowing the agent to bind the interstitial VEGF. When the complex intravasates (via a combination of lymphatic drainage and microvascular transport of macromolecules) and dissociates in the blood, VEGF is released and the VEGF concentration increases in the plasma. These results provide a new hypothesis on the kinetics of VEGF and on the VEGF distribution in the body caused by anti-angiogenic therapies, as well as their mechanisms of action and could help in designing anti-angiogenic therapies.

Keywords

angiogenesis; anti-VEGF; bevacizumab; anti-angiogenic therapy; mathematical model

Corresponding Author: Aleksander S. Popel, Department of Biomedical Engineering, Johns Hopkins University School of Medicine, 720 Rutland Avenue, 611 Traylor Research Building, Baltimore, MD 21205, USA. Telephone 410-955-6419, apopel@jhu.edu.

Conflict of Interest: The authors hereby declare no competing conflicts of interest.

Quick Guide To Equations And Assumptions

i. Key equations

The molecular-detailed compartmental model is described by non-linear ordinary differential equations based on the principles of chemical kinetics and biological transport (summarized in Supplement 1). The following example equation describes the change over time of the concentration of vascular endothelial growth factor $VEGF_{121}$ isoform in the interstitial space of the normal tissue, denoted by the subscript *N*. The blood compartment is denoted by the subscript *B*.

$$\begin{aligned}\frac{d[V_{121}]_N}{dt} &= q^N_{V121} - k_{on,V121,R1}[V_{121}]_N[R_1]_N + k_{off,V121R1}[V_{121}R_1]_N \\ &\quad - k_{on,V121,R2}[V_{121}]_N[R_2]_N + k_{off,V121R2}[V_{121}R_2]_N \\ &\quad - k_{on,V121,R1N1}[V_{121}]_N[R_1N_1]_N + k_{off,V121R1N1}[V_{121}R_1N_1]_N \\ &\quad - k_{on,V121,A}[V_{121}]_N[A]_N + k_{off,V121A}[V_{121}A]_N \\ &\quad - \left(\frac{k_L + k^{NB}_{pV}S_{NB}}{U_N}\right)\frac{[V_{121}]_N}{K_{AV,N}} + k^{BN}_{pV}\frac{S_{NB}}{U_N}\frac{U_B}{U_p}[V_{121}]_B\end{aligned}$$

The right hand side terms represent: secretion of $VEGF_{121}$ isoform (q_{V121}); binding to $VEGF_{121}$ to its receptors (VEGFR1 and VEGFR2) and to the complex VEGFR1/NRP1; binding of $VEGF_{121}$ to the anti-VEGF agent *A*; and the inter-compartmental transport of $VEGF_{121}$ by lymphatics (k_L) and microvascular permeability to macromolecules (k_p). $S_{N,B}$ and $K_{AV,N}$ represent the total surface of microvessels at the normal tissue/blood interface and the available volume fraction for $VEGF_{121}$ in the total volume U_N, respectively. The total volumes are denoted *U*. The subscript *p* in U_p denotes plasma as distinct from blood. Note that, with this nomenclature, the ratio U_p/U_B represents the available fluid volume fraction for $VEGF_{121}$ in the blood.

The injection of the anti-VEGF agent occurs after establishment of a physiological steady state (t<0). At t=0, the anti-VEGF agent is administered intravenously at a rate q_A for a duration $\Delta t_{infusion}$ (typically in minutes). The subscript *T* represents the tumor. The equation governing the change of the anti-VEGF agent concentration in the blood over time reads:

$$\begin{aligned}\frac{d[A]_B}{dt} &= q_A - c_A[A]_B - k^{BN}_{pV}\frac{S_{NB}}{U_p}[A]_B + \left(\frac{k_L + k^{NB}_{pV}S_{NB}}{U_B}\right)\frac{[A]_N}{K_{AV,N}} \\ &\quad - k^{BT}_{pV}\frac{S_{TB}}{U_p}[A]_B + k^{TB}_{pV}\frac{S_{TB}}{U_B}\frac{[A]_T}{K_{AV,T}} \\ &\quad - k_{on,V121,A}[V_{121}]_B[A]_B + k_{off,V121A}[V_{121}A]_B \\ &\quad - k_{on,V121,A}[V_{165}]_B[A]_B + k_{off,V165A}[V_{165}A]_B\end{aligned}$$

where q_A = total dose/($n \times \Delta t_{infusion}$) during the duration of each treatment $\Delta t_{infusion}$ and q_A = 0 for all other times (*n* = number of injections). The first two terms on the right-hand side are the intravenous infusion of anti-VEGF at a rate q_A and the clearance of anti-VEGF from the blood at a rate c_A. The next terms represent: drug extravasation; removal of anti-VEGF agent by lymphatics; and drug intravasation (when the inter-compartment transports are included). The last two terms describe the binding of the anti-VEGF agent to both VEGF isoforms.

As a final example, the change over time of the corresponding VEGF/anti-VEGF concentration in the normal tissue when the extravasation of the anti-VEGF agent is governed by

$$\frac{d[V_{121}A]_N}{dt} = k_{on,V121,A}[V_{121}]_N[A]_N - k_{off,V121A}[V_{121}A]_N - \left(\frac{k_L + k_{pV}^{NB} S_{NB}}{U_N}\right)\frac{[V_{121}A]_N}{K_{AV,N}} + k_{pV}^{BN}\frac{S_{NB}}{U_N}\frac{U_B}{U_p}[V_{121}A]_B$$

and is dependent on: $VEGF_{121}$ binding to the anti-VEGF agent; and transport of the VEGF/anti-VEGF complex between the compartments.

ii. Major assumptions

Our model does not represent a particular stage or type of cancer to keep the model general in light of the fact that bevacizumab is administered in primary and metastatic diseases and in adjuvant or neoadjuvant settings. Therefore, our tumor compartment can either be a primary tumor or the aggregate of metastases in tissue.

Because the simulation results for a smaller tumor (half the diameter of the tumor considered in this study) were not significantly different (both qualitatively and quantitatively – data not shown), our model does not consider the possible change in tumor volume that may result from the injection of the anti-VEGF agent for the duration of our simulations.

The degradation of VEGF by proteases is not currently included in the model. Effects of platelets and leukocytes as potential sites for sequestering VEGF, anti-VEGF and their products are not considered and should also be added in the future. We assume that only endothelial cells express VEGF receptors. Our model does not include the presence of receptors on the luminal surface of endothelial cells and the quantification of abluminal receptors has been estimated from previous studies.

The model does not include multimeric binding of the anti-VEGF or the ability of the anti-VEGF to bind to matrix-bound VEGF. We assume that the anti-VEGF has a half-life of 21 days. Its complexes formed by the binding of $VEGF_{121}$ or $VEGF_{165}$ are assumed to have the same half-lives since bound and free bevacizumab exhibit the same pharmacokinetic profile. The binding and unbinding rates of the anti-VEGF to VEGF are taken from the literature to be 9.2×10^4 $M^{-1}{\cdot}s^{-1}$ and 2.0×10^{-4} s^{-1} respectively, leading to a dissociation constant K_d of 2.2 nM. The above assumptions can be relaxed, if warranted by experimental data, within the framework of the model that is generally suitable for simulating anti-VEGF therapeutics.

Introduction

VEGF is a key factor in tumor angiogenesis, and it has become a major target of anti-angiogenic cancer therapy (1). A large body of evidence suggests that the free plasma VEGF concentration is elevated several fold in cancer patients compared to healthy subjects (2). Therapies targeting VEGF have shown promising results in cancer. Bevacizumab (Avastin®, Genentech Inc., South San Francisco, CA), a recombinant humanized monoclonal antibody to VEGF, has demonstrated efficacy in colorectal cancer, non-small cell lung cancer, breast cancer, renal cell carcinoma and glioblastoma. The drug has been approved by the Food and Drug Administration for these indications under certain conditions in combination with chemotherapeutic agents and is being tested for other types of cancer and other conditions in numerous clinical trials.

Despite the growing clinical applications of bevacizumab, the mechanism of action of this anti-VEGF agent and that of other anti-VEGF large molecules is not sufficiently understood (3). Specifically, two important questions remain: whether the drug acts by sequestering

VEGF in the blood, tumor interstitium or both; and whether, as a result, the VEGF concentration in these compartments is reduced to 'normal' levels. Answering these questions would significantly contribute to understanding the mechanism of action not only at the molecular level, but also at the levels of tissue, organ and whole body and would help in the design of anti-VEGF agents. Gordon et al. reported that the intravenous injection of bevacizumab led to an increase in serum total VEGF in clinical trials while free VEGF concentration was reduced (4). Since then, other groups have reported counterintuitive increases in the plasma VEGF level following bevacizumab administration (5-7). In the ocular setting, Campa et al. reported that intravitreal bevacizumab injection increased the VEGF concentration in the aqueous humor (8). Several hypotheses have been formulated to explain this phenomenon. Hsei et al. have suggested that the clearance of complexed VEGF is lower than that of free VEGF in rats and hypothesized that this lower clearance could explain the accumulation of total VEGF in serum (9). Other groups have suggested alternate pathways activated by the injection of bevacizumab, such as: accumulation of hypoxia-inducible factor leading to an increase of VEGF in serum; or secondary macular edema for the eye (8,10,11). Loupakis et al. immunodepleted plasma to remove bevacizumab and bevacizumab-VEGF complexes, and found that plasma free VEGF was significantly reduced after bevacizumab administration (12); this methodology helps to circumvent the problem that the ELISA method used in a number of studies cannot distinguish between free and total (including bevacizumab-bound) VEGF. The results of the study corroborate an earlier proposal by Christofanilli et al. (13) that free VEGF can serve as a surrogate marker.

Systems biology approaches, and specifically computational and mathematical modeling, are emerging as powerful tools in fundamental studies of cancer and design of therapeutics (14,15). To better understand VEGF distribution in the body, we have built a three-compartment model composed of normal (healthy) tissue, blood and tumor (16). In this study, we have extended our computational model by including an anti-VEGF agent delivered by the intravenous infusion (i.e., into the blood compartment). The model describes the effect of such administration on the VEGF distribution in the blood, normal and diseased tissues. Our goal is to understand how the distribution of VEGF, anti-VEGF agent and their products changes following the agent administration; in particular, we will investigate whether the plasma VEGF level increases or decreases following an intravenous injection of the anti-VEGF agent.

Even though the results are presented using the parameters for bevacizumab, the model can be applied to other anti-VEGF agents. One such agent is aflibercept or VEGF Trap (Regeneron Pharmaceuticals Inc., Tarrytown, NY), a soluble humanized VEGF receptor protein designed to bind all VEGF-A isoforms and placental growth factor (PlGF). This fusion protein serves as a soluble decoy receptor and is currently in clinical trials.

Our model includes two VEGF-A isoforms ($VEGF_{121}$ and $VEGF_{165}$), as well as VEGF receptors (VEGFR1 and VEGFR2) and the co-receptor neuropilin-1 (NRP1). In this study, we assume that VEGFR1, VEGFR2 and NRP1 are present only on the abluminal surface of the endothelial cells. The transcapillary microvascular permeability for the diffusible molecules (VEGF, anti-VEGF and the VEGF/anti-VEGF complex) is included, as well as lymphatic drainage from the interstitial space into the blood compartment. The model equations are presented in the Supplemental Information (Supplement 1).

Materials And Methods

Most of the parameters for the anti-VEGF agent were taken from published data on bevacizumab. We assume a half-life of 21 days (4) for the anti-VEGF whether unbound or bound to $VEGF_{121}$ or $VEGF_{165}$, as bound and free bevacizumab exhibit the same

pharmacokinetic profile (9). Kinetic parameters (k_{on}, k_{off}) for the binding and unbinding of the anti-VEGF to the vascular endothelial growth factor were taken to be 9.2×10^4 $M^{-1} \cdot s^{-1}$ and 2.0×10^{-4} s^{-1} respectively, leading to a dissociation constant K_d of 2.2 nM (17).

Experiments have shown that bevacizumab may have multimeric binding to VEGF (9,18) and can bind to extracellular matrix-sequestered VEGF (19). For simplicity purposes, we limit our model to monomeric binding to VEGF and neglect binding to VEGF sequestered by the extracellular matrix; these can be included when quantification of binding sites and the kinetics become available. Bevacizumab has also been reported to alter the VEGF-dependent microvascular permeability to soluble molecules (20). As a first approximation, we assume that the geometry of each tissue and the capillary density remain constant in the course of our simulations, i.e., we do not include tissue remodeling after the injection of the anti-VEGF agent. Although it may be important, the inclusion of tissue remodeling would take the model beyond the scope of this study but could be of interest for further studies. This model does not include VEGF receptors on the luminal side of endothelial cells that have not been experimentally characterized, but we have recently shown how such expression would alter the VEGF distribution (21).

Note that the simulations are not aimed at representing a particular type or stage of cancer, recognizing that VEGF-neutralizing agents may be administered in cases of both metastatic and primary tumors. Thus, in the model the tumor compartment can represent either an aggregate volume of metastases or a primary tumor. Due to the wide range of possibilities that could be represented for different types and stages of cancer, we adopt the parameters for this compartment from our previous study (16) and conduct a sensitivity study to ascertain that our qualitative conclusions are not dependent on the choice of parameters.

For each simulation, the system was first equilibrated at a baseline for a cancer patient with tumor before the injection of the VEGF-neutralizing agent. At time zero, intravenous infusion of the anti-VEGF agent begins and delivery to the blood compartment continues as a slow infusion for 90 minutes. We considered two treatment regimens: a single-dose treatment of 10 mg/kg or 10 consecutive daily doses of 1 mg/kg (metronomic therapy).

The parameters and their assigned numerical values are summarized in Supplement 3. The equations governing the three-compartment VEGF transport system have been described in our previous papers (16, 21) and can be found in Supplement 1. We have also added equations to describe the interactions and inter-compartmental transport of the anti-VEGF molecule (Equations (S.30) to (S.38)).

Results

Experiments demonstrate an inverse relationship between microvascular permeability and the size of a molecule (molecular weight or Stokes-Einstein radius) (22-24). Therefore, in the absence of active transport, large proteins such as anti-VEGF agents (150 kDa for bevacizumab and 110 kDa for aflibercept) should extravasate relatively slowly. In apparent agreement with this, the level of bevacizumab following an intravenous injection has been observed to be several times lower in normal tissues (25) and in tumors (19) than in the blood. However, little is known about what role, if any, the extravasation of an anti-VEGF agent may play in the therapeutic mechanism. To address this issue, we considered two computational scenarios: in the first, the anti-VEGF agent is constrained in the blood compartment (negligible extravasation); in the second, the extravasation of the anti-VEGF agent is included.

Plasma free VEGF is predicted to decrease following intravenous injection of an anti-VEGF agent confined to the blood compartment (no extravasation)

Changes in plasma and tissue free VEGF are summarized in Figure 1A for a single injection (10 mg/kg) and Figure 1C for metronomic therapy (1 mg/kg daily for 10 days), i.e., repeated lower doses over a longer period of time (26). Total amount of drug injected is the same in both scenarios.

If the anti-VEGF agent is confined to the blood compartment, a single injection causes the concentration of free VEGF (i.e., not bound to anti-VEGF) in plasma to decrease precipitously by 98.4% (Figure 1A, dashed line; minimum as the infusion ends), as the anti-VEGF agent binds to VEGF available in plasma. However, this is not predicted to significantly affect the free VEGF level in the healthy tissue (maximum 0.1% drop at 9 hours – solid line) or the free VEGF level in the tumor compartment (maximum 0.2% drop at 30 hours – dotted line). The free anti-VEGF agent saturated the blood (Figure S1A) and reached a maximum of ~1.7 μM in plasma (~88 μg/mL plasma) at the end of the infusion, which corresponds to the total injected amount of the 150-kDa agent distributed in the volume of plasma for a 70-kg patient. The VEGF/anti-VEGF complex reached its maximum concentration in the blood (~2.1 nM) after about 12 days (Figure S2A). The total (free and bound to the anti-VEGF agent) VEGF concentration is typically what is measured by VEGF ELISA methods (see Supplement 2 for a compilation of experimental data on free/total VEGF changes following bevacizumab administration). Our results show a 100 to a 1,000-fold difference between free VEGF concentration (Figure 1) and the concentration of VEGF bound to the anti-VEGF (Figure S2). Because of this difference in magnitude, the unbound VEGF concentration represents only a small percentage of the total VEGF concentration, and thus Figure S2 also illustrates the total VEGF concentration profile.

For metronomic therapy (lower daily dose of 1 mg/kg over 10 days), the free VEGF in plasma declines 86.8% following the first infusion, but is predicted to reach a pseudo-steady state after multiple infusions (Figure 1C – dashed line). The concentration of free VEGF returned to its baseline level within three weeks once the treatment was stopped. Metronomic therapy showed delayed and lowered maximum levels of anti-VEGF compared to the single-dose regimen (Figure S1C vs. S1A); although the half-life of the anti-VEGF agent is relatively long, it is being cleared from plasma continuously. The VEGF/anti-VEGF complex (and therefore the total VEGF concentration) reached its maximum about a week later than for the single dose (Figure S2C vs. Figure S2A).

For an anti-VEGF agent that extravasates, plasma free VEGF is predicted to first decrease and then increase above the baseline level

As for a non-extravasating anti-VEGF agent (Figure 1A), plasma free VEGF decreased (97.0% drop in the first 45 minutes) following administration of anti-VEGF that can extravasate (Figure 1B, dashed line), as the agent binds to available free VEGF. In this case, however, VEGF concentration then rebounded to 41.1 pM (a 9.1-fold increase over baseline) after about 1 week. Unlike the no-extravasation case where the concentration returned to baseline after three weeks, the free VEGF concentration in plasma was predicted to remain significantly elevated after three weeks (40.5 pM, 9-fold the baseline level). The free VEGF concentration in the normal (solid line) and tumor (dotted line) tissues both also showed an initial transient decrease (58.5% and 88.9% respectively), followed by a slight rebound, reaching steady-states 6.8% and 69.7% below baseline, respectively. This could be due to the long half-life of the anti-VEGF agent (21 days) as compared to the characteristic times of clearance, binding affinities, and internalization rates of VEGF receptors. This may suggest that an important if not the primary action of the anti-VEGF agent is to deplete the

tumor VEGF after the anti-VEGF extravasation. Interestingly, the increase of free VEGF in plasma is also predicted even in the absence of a tumor compartment (data not shown).

Figure S1B shows the dynamic response of the free anti-VEGF agent concentration. Upon injection, the free anti-VEGF concentration at first increases but then decreases rapidly within the next 12 hours as it travels to the normal and tumor tissues. Interestingly, the free anti-VEGF concentrations in the blood and in the tumor were almost identical. This was mainly due to the higher microvascular permeability and the absence of functioning lymphatics in the tumor. The formation of the VEGF/anti-VEGF complex (and the total VEGF concentration) reached a maximum after about 4 days and was significantly higher in the tumor than in the other compartments due to higher VEGF concentrations (Figure S2B).

In metronomic therapy (Figure 1D), similar results were observed. The free VEGF concentration decreased in the plasma upon the anti-VEGF injection then rebounded and increased further after each injection (dashed line). In the healthy and tumor compartments (solid and dotted lines, respectively), a decrease in the free VEGF concentration was observed, followed by a rebound effect without exceeding their respective baseline levels. In all three compartments, the free VEGF concentrations are predicted to reach a steady state at the end of the 10 days of treatment and then remain almost constant (varying within a small range) over the duration of the experiment: the free VEGF level in the tumor was significantly decreased (~70.1%), whereas that in the plasma was significantly increased (by 8 fold) as compared to the baseline. Although the rebound in free VEGF in plasma occurred after 45 minutes, if we limit the duration of the treatment to 45 minutes instead of 90 minutes, the rebound still happens (data not shown). The free anti-VEGF concentration peaked following each injection, reaching an overall maximum after 10 days of about half that for the single-dose treatment (Figure S1D vs. S1B). Interestingly, more VEGF/anti-VEGF complex was formed in the tumor (dotted line) than in the blood (dashed line) or in the normal tissue (solid line), regardless of the regimen (Figures S2B and S2D, for single-injection and metronomic therapy, respectively). This also means that the total VEGF concentration was higher in the tumor than in the blood or the normal tissue.

Formation of the VEGF/anti-VEGF complex mediates the depletion of VEGF from the tumor

The changes in VEGF concentrations induced by the anti-VEGF agent can be interpreted by a detailed study of the movement of VEGF and anti-VEGF between the three compartments. We define the net flow for each molecule as the difference between the inter-compartmental flows of that molecule (in moles per unit time) entering and leaving the compartment. For example, the net inter-compartmental flow of VEGF in the normal tissue is the difference between VEGF influx (by extravasation) and VEGF leaving the compartment (by intravasation and lymphatic drainage). With this metric, any negative net flows represent flows of diffusible molecules traveling from the blood into the normal tissue or the tumor compartment, while positive net flow illustrates the flow of molecules entering the blood compartment. To visualize the relative effects, we plotted the net inter-compartmental flows on the same graph. Figure 2 illustrates the net flows for the free VEGF, free anti-VEGF agent and VEGF-anti-VEGF complex for the few hours following the anti-VEGF agent intravenous injection.

The anti-VEGF net flows (light gray) increased significantly during the first 6 to 12 hours in the normal (solid line) and tumor tissues (dotted line), showing extravasation of the anti-VEGF agent followed by subsequent binding to VEGF once in the normal or tumor tissues. For example, within 4-5 hours, 58% of VEGF in the healthy tissue has become complexed with the anti-VEGF agent (Figure 1B). This is mainly due to the fact that the dose of the anti-VEGF agent injected is several orders of magnitude higher than the free VEGF concentration in the blood and, therefore, the anti-VEGF saturates the plasma upon

injection. This concentration difference is counteracted by the microvascular permeability of the high molecular-weight (150 kDa) anti-VEGF being lower than that of VEGF (~45 kDa).

The net inter-compartmental flow of the VEGF/anti-VEGF complex reveals that effectively, there is a net flow of complex intravasating from the normal tissue. This result suggests that the role of the anti-VEGF is to deplete VEGF from the interstitial spaces of the normal tissue and the tumor in the form of a complex.

The VEGF distribution is modified by the injection of the anti-VEGF agent

Relative VEGF distribution changes in normal tissue, blood, and tumor upon administration of the anti-VEGF agent (Figure 3). In the blood (middle graph), there is no significant amount of free VEGF since most of it is complexed with the anti-VEGF agent. In the normal and tumor tissues (top and bottom graphs, respectively), most VEGF is complexed with the anti-VEGF agent (light gray region). The decrease in the relative amount of unbound VEGF in each compartment (black region), however, is mostly due to increase in total VEGF, due to the formation of VEGF/anti-VEGF complex (Figure S3). In normal tissue, unbound VEGF declines only transiently; in tumors, there is a steady-state decline, where VEGF is much less bound to its receptors (drop by 48% – dark gray region) and less sequestered in the matrix (drop by 69% – white region) than before injection.

The administration of the anti-VEGF agent significantly modifies the VEGFR1 and NRP1 occupancies in the tumor

In keeping with the predicted effect on unbound VEGF (Figure 1), occupancy of the receptors in normal tissue was only transiently altered by the administration of the anti-VEGF agent (Figure 4 – solid line), while the VEGFR1 and NRP1 occupancies (top and bottom graphs) in the tumor were significantly decreased (from 31% to about 10%, and 35% to about 18% for VEGFR1 and NRP1, respectively) and remained fairly unchanged over the course of the experiment (dotted lines). Changes in VEGFR2 occupancy appeared less significant (middle graph), due to the saturation of tumor VEGFR2 by cell-surface association of VEGF-bound neuropilin-1; we assume 10-fold higher neuropilin-1 expression on tumor endothelial cell surfaces than that of VEGFR2 in our model, and 10-fold higher than on normal tissue endothelial cells. The effect of parameters on the qualitative results of the study is discussed below. VEGFR2 occupancy after the anti-VEGF administration does not significantly change in the tumor compartment as compared to baseline (50% and 100% ligated in single and metronomic therapies, respectively).

Discussion and Conclusion

The mechanism of action of bevacizumab has been commonly accepted as its binding to the VEGF protein resulting in inhibition of angiogenesis. However, recent analysis points out that “while the molecular targets for anti-VEGF therapy with large molecules are identified, the mechanism of action, that is, how an anti-VEGF approach can exert single agent activity in some cancers and augment the efficacy of conventional chemotherapy, is not well understood” (3). It is important to know if the binding takes place in the blood or tumor, and how it might affect the signaling via VEGF receptors. Our systems biology study is aimed at clarifying these questions.

Our model provides insights into the potential mechanisms of action of anti-VEGF agents. However, the implications of current model assumptions need to be considered. Our conclusions might depend on the tumor microenvironment, specifically on the VEGF receptor expression on endothelial, cancer, and stromal cells. VEGF receptor expression in vivo has not been quantitatively characterized. However, our sensitivity analysis where we

vary some of these factors shows that the qualitative conclusions remain unchanged (data not shown). A decrease in VEGF degradation by proteases may also contribute to increasing the VEGF level in the plasma. It is also possible that VEGF molecules are released from platelets that have a very high VEGF concentration (27,28). Proteases or platelets are not included in the present model but should be added as more quantitative data become available.

Table S1 (Supplemental data) summarizes changes of VEGF levels following a bevacizumab injection found in the literature. In 2001, Gordon et al. reported that serum total VEGF level increased while serum free VEGF level decreased. They suggested that this behavior could be the result of VEGF synthesis or a decrease in VEGF clearance due to the complexation with the VEGF antibody. A year later, Hsei et al. performed an experiment on rats to assess this issue and showed that the VEGF clearance decreased about 3 fold in the presence of bevacizumab, while the clearance and terminal half-life of bevacizumab were not significantly changed by the complexation (9). However, more recently, a similar behavior was seen following the treatment of VEGF tyrosine kinase inhibitors (11, 12, 29), leading to the possibility that the decrease in VEGF clearance may not be sufficient to explain the counterintuitive phenomenon. Importantly, Loupakis et al. showed that immunodepleted blood samples revealed a significant decrease of VEGF after bevacizumab injection (12). Our model can assess both free and total VEGF, and shows that free VEGF (and total VEGF) can increase or decrease depending on the ability for bevacizumab and its complex to extravasate. It would be of interest to add platelets and leukocytes to our compartment model that can sequester VEGF and investigate if that could provide more insights into the phenomenon.

Note that except for glioblastomas where bevacizumab has indicated use as a single agent, bevacizumab has been approved by the FDA as a combination therapy for other cancers. Our simulations using a quantitative molecular-based pharmacokinetic model provide a possible characterization for the mechanism of action of the anti-VEGF agents. In particular, we predict that the mechanism of action of anti-VEGF agents includes depleting the tumor interstitial VEGF, and not the blood VEGF, which increases in qualitative agreement with several experimental studies. The concentration of the anti-VEGF agent after intravenous injection is six orders of magnitude higher than that of the VEGF present in the plasma (micromolar levels in Figure S1 for the anti-VEGF agent as compared to picomolar levels in Figure 1 for VEGF). Therefore, upon injection, most of the free VEGF in the plasma binds to the anti-VEGF molecules that saturate the blood. Despite the relatively low microvascular permeability for the anti-VEGF agent, the anti-VEGF molecules extravasate (Figure 2) and bind to free VEGF in the interstitial space (Figures 1, 3 and S2). This leads to a significant decrease of free VEGF in the tumor (Figure 2), leading to a decrease in ligation of two receptors (VEGFR1 and NRP1). However, the simulations predict that the VEGFR2 remains nearly fully ligated in the tumor compartment (Figure 4). These results are not obvious: the anti-VEGF agent has a high molecular weight (about 150 kDa) so one would not expect the microvascular permeability to play a very important role for the anti-VEGF agent transport. Our model shows that, on the contrary, the inclusion of inter-compartment transport is crucial in order to understand the mechanism of action of the anti-VEGF agent. Even the small fraction of anti-VEGF agent that traverses the endothelial barrier (into the normal tissue or tumor) affects VEGF level in the interstitium, especially in the tumor (Figure 1). Our model reveals that this phenomenon is intrinsic to the system and does not require any further hypotheses regarding the VEGF system and/or the drug; however, the processes hypothesized by other groups may also play a role in the overall mechanism of action. Our computational model suggests that it would be of great interest to design an experiment where tracking of the binding of the drug and tracking of the flows of VEGF, anti-VEGF and VEGF/anti-VEGF complex would be included.

We asked whether the drug acts by sequestering VEGF in the blood, tumor interstitium or both, and whether, as a result, the VEGF concentration in these compartments is reduced to 'normal' levels. Our model shows that the drug may act by depleting VEGF from the tumor interstitium, rather than depleting VEGF in the blood where the concentration decreases transiently followed by a several-fold sustained increase. The model also shows that the VEGF concentration in the tissue compartments are not reduced to the 'normal' levels but instead reach a new pseudo-steady state, close to the level of VEGF in the normal tissue prior to injection. We hope that these results will motivate new experiments in order to investigate the binding and flows in the VEGF system under an anti-VEGF treatment and that our model will initiate new investigations for therapeutic purposes and drug design.

Supplementary Material

Refer to Web version on PubMed Central for supplementary material.

Acknowledgments

Financial support This work was supported by NIH grants R01 CA138264 (ASP) and R00 HL093219 (FMG).

References

1. Gaur P, Bose D, Samuel S, Ellis LM. Targeting tumor angiogenesis. Semin Oncol. 2009; 36(2 Suppl 1):S12–9. [PubMed: 19393831]
2. Kut C, Mac Gabhann F, Popel AS. Where is VEGF in the body? A meta-analysis of VEGF distribution in cancer. Br J Cancer. 2007; 97(7):978–85. [PubMed: 17912242]
3. Grothey A, Galanis E. Targeting angiogenesis: progress with anti-VEGF treatment with large molecules. Nat Rev Clin Oncol. 2009; 6(9):507–18. [PubMed: 19636328]
4. Gordon MS, Margolin K, Talpaz M, et al. Phase I safety and pharmacokinetic study of recombinant human anti-vascular endothelial growth factor in patients with advanced cancer. J Clin Oncol. 2001; 19(3):843–50. [PubMed: 11157038]
5. Segerstrom L, Fuchs D, Backman U, Holmquist K, Christofferson R, Azarbayjani F. The anti-VEGF antibody bevacizumab potently reduces the growth rate of high-risk neuroblastoma xenografts. Pediatr Res. 2006; 60(5):576–81. [PubMed: 16988184]
6. Willett CG, Boucher Y, Duda DG, et al. Surrogate markers for antiangiogenic therapy and dose-limiting toxicities for bevacizumab with radiation and chemotherapy: continued experience of a phase I trial in rectal cancer patients. J Clin Oncol. 2005; 23(31):8136–9. [PubMed: 16258121]
7. Yang JC, Haworth L, Sherry RM, et al. A randomized trial of bevacizumab, an anti-vascular endothelial growth factor antibody, for metastatic renal cancer. N Engl J Med. 2003; 349(5):427–34. [PubMed: 12890841]
8. Campa C, D'Angelo S, Incorvaia C. Comment of article by Matsumoto Y. Retina. 2008; 28(5):782. author reply -3. [PubMed: 18463528]
9. Hsei V, Deguzman GG, Nixon A, Gaudreault J. Complexation of VEGF with bevacizumab decreases VEGF clearance in rats. Pharm Res. 2002; 19(11):1753–6. [PubMed: 12458683]
10. Matsumoto Y, Freund KB, Peiretti E, Cooney MJ, Ferrara DC, Yannuzzi LA. Rebound macular edema following bevacizumab (Avastin) therapy for retinal venous occlusive disease. Retina. 2007; 27(4):426–31. [PubMed: 17420693]
11. Yang JC. Bevacizumab for patients with metastatic renal cancer: an update. Clin Cancer Res. 2004; 10(18 Pt 2):6367S–70S. [PubMed: 15448032]
12. Loupakis F, Falcone A, Masi G, et al. Vascular endothelial growth factor levels in immunodepleted plasma of cancer patients as a possible pharmacodynamic marker for bevacizumab activity. J Clin Oncol. 2007; 25(13):1816–8. [PubMed: 17470880]
13. Cristofanilli M, Charnsangavej C, Hortobagyi GN. Angiogenesis modulation in cancer research: novel clinical approaches. Nat Rev Drug Discov. 2002; 1(6):415–26. [PubMed: 12119743]

14. Anderson AR, Quaranta V. Integrative mathematical oncology. Nat Rev Cancer. 2008; 8(3):227–34. [PubMed: 18273038]
15. Byrne HM. Dissecting cancer through mathematics: from the cell to the animal model. Nat Rev Cancer. 2010; 10(3):221–30. [PubMed: 20179714]
16. Stefanini MO, Wu FT, Mac Gabhann F, Popel AS. A compartment model of VEGF distribution in blood, healthy and diseased tissues. BMC Syst Biol. 2008; 2:77. [PubMed: 18713470]
17. Liang WC, Wu X, Peale FV, et al. Cross-species vascular endothelial growth factor (VEGF)-blocking antibodies completely inhibit the growth of human tumor xenografts and measure the contribution of stromal VEGF. J Biol Chem. 2006; 281(2):951–61. [PubMed: 16278208]
18. Rudge JS, Holash J, Hylton D, et al. Inaugural Article: VEGF Trap complex formation measures production rates of VEGF, providing a biomarker for predicting efficacious angiogenic blockade. Proc Natl Acad Sci U S A. 2007; 104(47):18363–70. [PubMed: 18000042]
19. Nagengast WB, de Vries EG, Hospers GA, et al. In vivo VEGF imaging with radiolabeled bevacizumab in a human ovarian tumor xenograft. J Nucl Med. 2007; 48(8):1313–9. [PubMed: 17631557]
20. Pham CD, Roberts TP, van Bruggen N, et al. Magnetic resonance imaging detects suppression of tumor vascular permeability after administration of antibody to vascular endothelial growth factor. Cancer Invest. 1998; 16(4):225–30. [PubMed: 9589031]
21. Stefanini MO, Wu FT, Mac Gabhann F, Popel AS. The presence of VEGF receptors on the luminal surface of endothelial cells affects VEGF distribution and VEGF signaling. PLoS Comput Biol. 2009; 5(12):e1000622. [PubMed: 20041209]
22. Michel CC, Curry FE. Microvascular permeability. Physiol Rev. 1999; 79(3):703–61. [PubMed: 10390517]
23. Schmittmann G, Rohr UD. Comparison of the permeability surface product (PS) of the blood capillary wall in skeletal muscle tissue of various species and in vitro porous membranes using hydrophilic drugs. J Pharm Sci. 2000; 89(1):115–27. [PubMed: 10664544]
24. Yuan F, Dellian M, Fukumura D, et al. Vascular permeability in a human tumor xenograft: molecular size dependence and cutoff size. Cancer Res. 1995; 55(17):3752–6. [PubMed: 7641188]
25. Lin YS, Nguyen C, Mendoza JL, et al. Preclinical pharmacokinetics, interspecies scaling, and tissue distribution of a humanized monoclonal antibody against vascular endothelial growth factor. J Pharmacol Exp Ther. 1999; 288(1):371–8. [PubMed: 9862791]
26. Kerbel RS, Kamen BA. The anti-angiogenic basis of metronomic chemotherapy. Nat Rev Cancer. 2004; 4(6):423–36. [PubMed: 15170445]
27. Klement GL, Yip TT, Cassiola F, et al. Platelets actively sequester angiogenesis regulators. Blood. 2009; 113(12):2835–42. [PubMed: 19036702]
28. Peterson JE, Zurakowski D, Italiano JE Jr, et al. Normal ranges of angiogenesis regulatory proteins in human platelets. Am J Hematol. 2010; 85(7):487–93. [PubMed: 20575035]
29. Motzer RJ, Michaelson MD, Redman BG, et al. Activity of SU11248, a multitargeted inhibitor of vascular endothelial growth factor receptor and platelet-derived growth factor receptor, in patients with metastatic renal cell carcinoma. J Clin Oncol. 2006; 24(1):16–24. [PubMed: 16330672]

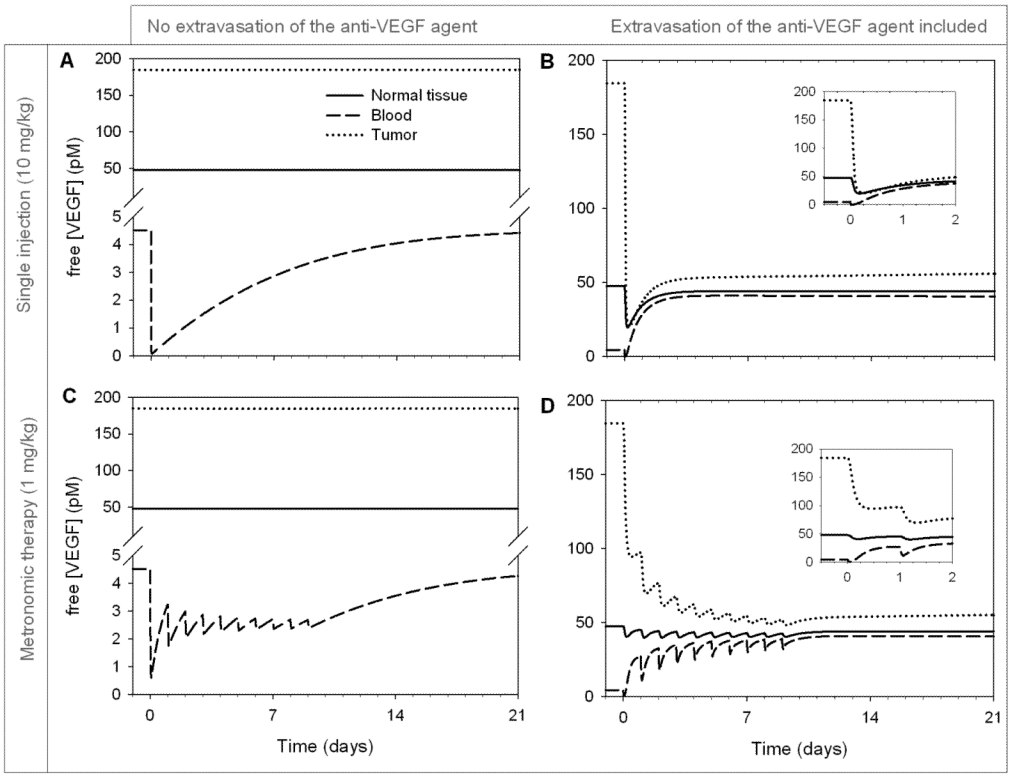

Figure 1. Free VEGF concentration profiles following the intravenous injection of an anti-VEGF agent

A-B. Single injection (10 mg/kg), **C-D**. Daily injection of 1 mg/kg for 10 days (metronomic therapy). 1 pM VEGF equivalent to 24 pg/mL total blood. Solid line: normal tissue; dashed line: blood; dotted line: tumor.

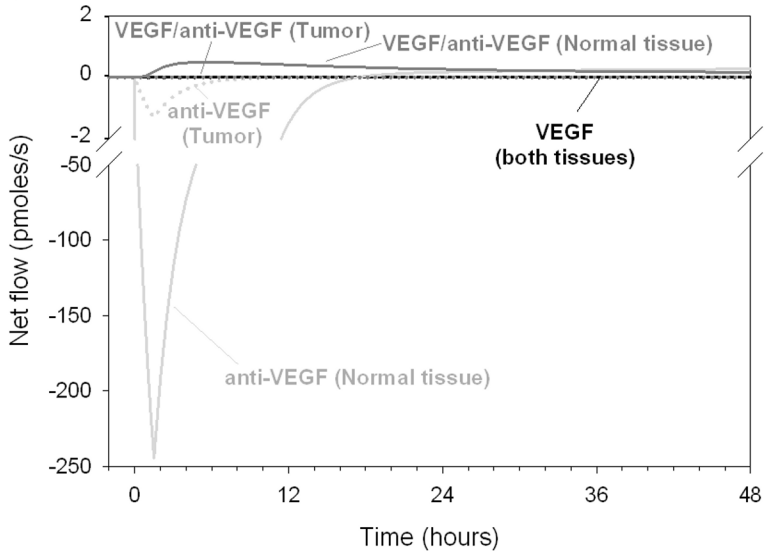

Figure 2. Net inter-compartmental flows of VEGF, anti-VEGF and VEGF/anti-VEGF complex
Solid line: normal tissue; dotted line: tumor. Black: free VEGF; light gray: anti-VEGF agent; dark gray: VEGF/anti-VEGF complex (also total VEGF).

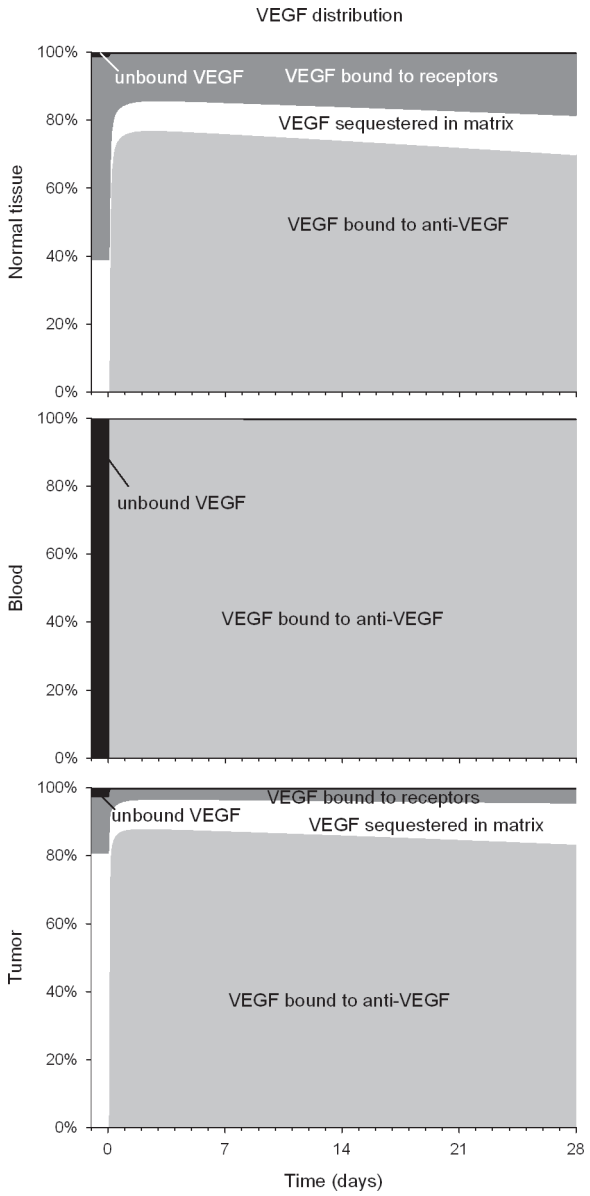

Figure 3. Relative VEGF distribution profiles in normal, blood and tumor tissues

Percentage of VEGF bound to the anti-VEGF agent, free, bound to the receptors and sequestered in the extracellular matrix. From top to bottom: normal tissue, blood, tumor. Light gray: VEGF bound to anti-VEGF (VEGF/anti-VEGF complex); white: VEGF bound to the extracellular matrix; dark gray: VEGF bound to receptors; black: unbound VEGF.

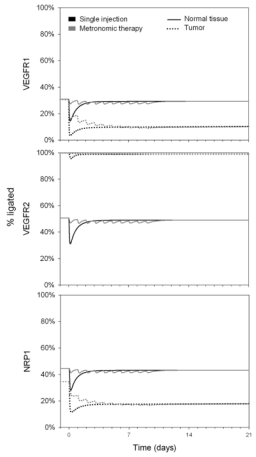

Figure 4. VEGF receptor occupancy profiles

Percentage of ligated and unligated receptors. **A**. VEGFR1, **B**. VEGFR2, **C**. NRP1. Solid line: normal tissue; dotted line: tumor. Black: single injection; gray: metronomic therapy.